Chapter 3

Deformation Regimes for Sphere-Plane Contact: Revisiting Tabor's Criteria for Differential Hardness

Giuseppe Pintaude

Additional information is available at the end of the chapter

http://dx.doi.org/10.5772/intechopen.72642

Abstract

This chapter presents an update of theories involving the differential hardness problem, starting from the hypothesis made by Tabor for the contact between a sphere and a plane. In this way, the reader interested in problems affected directly by these formulations, such as contact area and contact fatigue, can take part of a fundamental theoretical basis to perform investigations in this field.

Keywords: differential hardness, sphere-plane contact, deformation regimes

1. Introduction

The contact mechanics, a branch of structural mechanics developed by the German physicist Heinrich Rudolf Hertz, describes the stresses and strains associated with a surface. His 1882 work, "Ueber die Berührung elastischer fester Körper" ("On the Contact Elastic Solid") is considered the starting point of this branch of science [1].

The solutions presented by Hertz do not involve friction; therefore, the bodies do not experience adhesion, and they are associated with purely elastic deformation field. The advancing in contact mechanics for modeling different deformation regimes depended on the development of computational simulation tools, especially the finite element method (FEM). In this sense, Mackerle [2] presented a summary on the use of FEM for indentation problems, a specificity of contact mechanics. In a period of 4 years, this author reported 187 references using FEM for a better understanding of indentation phenomena.

An immediate finding of this list of articles is that the contact stress distribution depends on the geometry of the bodies and the contact between a sphere and a plane is always the first approach for that, given the amount of engineering systems that can be associated with this kind of system. One of them is the hardness testing, wherein different scales are composed of this geometry, such as Brinell [3] and Rockwell B [4].

A very important aspect of the reliability of the hardness testing is to ensure that the plastic deformation occurs in the tested body, while only small deformations are allowed on the sphere. This warranty is given by the difference in hardness between the sphere and the tested body, which can be called differential hardness. Tabor [5] described an analytical estimate of what would be necessary for differential hardness. For that purpose, Tabor made use of some nontrivial simplifications, deserving to be detailed.

In this context, this book chapter intends to present an update of the theories involving the problem of differential hardness from the presentation of the assumptions made by Tabor to the initial problem, involving concepts of elasticity and plasticity. Thus, the tribology student interested in issues directly affected by these formulations, such as contact area calculation and contact fatigue, can find a fundamental theoretical basis for conducting investigations in this field of knowledge.

2. Differential hardness: Tabor's model

As the force applied during a hardness test is increased, the tested material passes to experience different regimes of deformation. Initially, Tabor [5] identified three regimes: elastic, elastic-plastic, and fully plastic. **Figure 1** shows these regimes schematically.

By measuring the hardness of a material, one should ensure that it is subject to full plasticity. Therefore, load values should be sufficient for the ratio between the mean contact pressure (which may be equivalent to the hardness (H)) and the material yield stress (Y) which exceeds a typical value. The relationship between the mean pressure and the yield stress is defined as the constraint factor (C (= H/Y)).

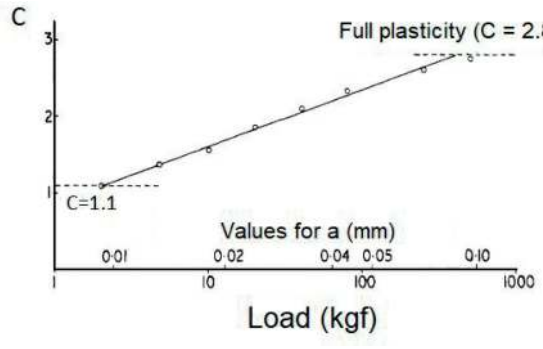

Figure 1. Deformation regimes under sphere-plane contact (Adapted from [5]).

On the other hand, if the sphere cannot experience plasticity, the deformation seen by the ratio of the mean contact pressure and yield stress must be restricted to a certain value. Thus, using the values for C shown in **Figure 1**, Tabor [5] calculated the differential hardness required for a sphere as follows:

$$p_m \approx 2.8Y_M \geq 1.1Y_B \therefore Y_M \geq 0.4Y_B \quad (1)$$

where Y_M is the yield stress of metal and Y_B is the yield stress of sphere.

If the material hardness has equivalency to the yield stress, the sphere must be 2.5 times harder than the tested body. As an example, Tabor describes a sphere of quenched and tempered steel, with typically 900 HV; for this case, it could be used to test materials with a 400 HV maximum.

The next items will be devoted for detailing the values used by Tabor for each regime—beginning of elastic-plastic regime and full plasticity—and further advances in the literature, provided by the numerical simulation techniques.

3. Yielding inception

The imminence of plastic yielding shall be described with the use of a suitable criterion. The criteria commonly used for metals are Tresca and von Mises, which are equivalent only in few specific conditions. Regardless of these conditions, the result of applying both criteria indicates that a metal yields by the action of shear forces, which makes the maximum shear stress significant to know. In a sphere-plane contact, the resulting shear stress can be described considering a normalized distance (z/a), where "z" is the depth below the surface and "a" is the contact radius established by Hertzian analytical solution.

The analytical equations necessary for calculating the maximum shear stress in the sphere-plane contact will not be presented here, but it is known that these are dependent upon Poisson's ratio of the material (ν) [6]. To describe a single curve as shown in **Figure 2**, it is necessary to set a value for this property, in which Tabor used 0.3 as a convenient value for most metals.

The curve in **Figure 2** with ν = 0.3 has the maximum value for the ratio τ_{max}/p_m of 0.468, which is normalized to a defined depth. In applying Tresca's criterion, one obtains [7]

$$p_m = \frac{\tau_{max}}{(\tau_{max}/p_m)} = \frac{Y}{2.(0.468)} = 1.07Y \quad (2)$$

Therefore, a relationship between the mean pressure and the yield stress of 1.07 is obtained, and this value was rounded to 1.1, as presented by Tabor for the formulation of the differential hardness, according to Eq. (1). For a material not yielding in a sphere-plane contact, the value of the applied load must correspond to a mean pressure not exceeding this value (see **Figure 1**).

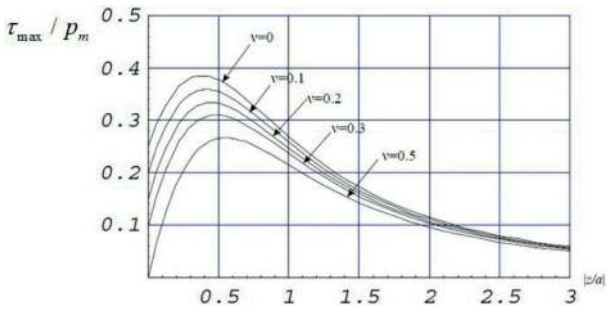

Figure 2. Distribution of normalized shear stress along normalized depth (z/a) under sphere-plane contact considering different values of Poisson's ratio (Adapted from [8]).

Changes in Poisson's ratio are sufficient to change both the magnitude of ratio τ_{max}/p_m and the location of this maximum value, as shown in **Figure 2**.

It is logical to expect that the relationship of Eq. (2) presents variations with ν. A series of equations have been proposed in the literature for that, having been summarized by Pintaude [9]. The author showed that five equations of the literature did not show great differences and that they can be divided into just two groups, in which some difference begins to be considered significant. This difference is associated with the given equivalence between the yield stress and the hardness, i.e., the constraint factor previously defined, which will be treated with utmost importance in the next section.

4. Full plasticity

The full plasticity regime associated with the contact between a sphere and a plane as defined by Tabor [5] presents no variations in the mean contact pressure; once this regime has been reached, this pressure has a defined value in relation to the yield stress of material. Tabor empirically found that the relationship between the hardness and the yield stress during a Brinell hardness test is 2.8; the value used by him to calculate the differential hardness ensures the plasticity of the material tested.

The use of a constant value to the constraint factor independent of system properties is a simplification in many ways, since a set of mechanical properties of materials dictates the behavior during the mechanical loading. Therefore, it is necessary to understand in a section, which occurs during this loading process, until the full plasticity is established for relatively large deformations/depths.

Figure 3 shows the definition of a plastic zone developed along an indentation process.

The contour of the plastic zone (c/a), shown in **Figure 3**, was modeled by Bishop et al. [11], which defines the limits of elastic-plastic deformation, being the same proportional to the ratio

http://dx.doi.org/10.5772/intechopen.72642

between the elastic modulus and the yield stress (E/Y). Thus, the same authors indicated that, by similarity, the constraint factor is also proportional to this ratio.

Since then, many models have been proposed to express the dependence of the factor C to the E/Y, and two currents are shown in **Figure 4** for a perfectly plastic material. One of them is due to Song and Komvopoulos (SK model) [12], in which Poisson's ratio is implicit into the value of E (one can consider ν as fixed), while Megalingam and Mayuram (model MM) [13] made this coefficient in its equation explicit. **Figure 4** compares the models for a fixed Poisson's ratio of 0.3.

It is found that SK and MM models differ more significantly for materials with relatively low values of E/Y and them approaching to 2.8 (used by Tabor) as E/Y increases.

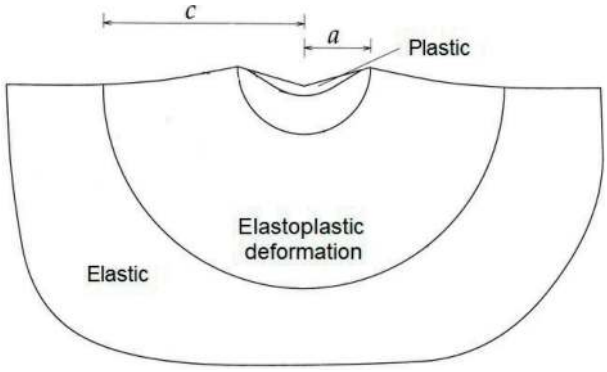

Figure 3. Plastic zone definition during an indentation process. Contours indicate the limits for deformation regimes (Adapted from [10]). Caption: a = contact radius and c = radius of plastically affected zone.

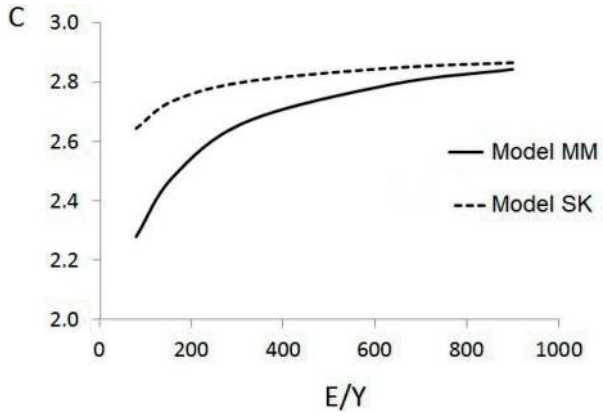

Figure 4. Variation of constraint factor with ratio E/Y following models SK [12] and MM [13], for a material with Poisson's ratio of 0.3.

The work-hardening effects could be added to the results of **Figure 4**, but before checking it is important to discuss the failure of **Figure 1** for describing the behavior of a material at high loads, which produce consequently large contact radii.

A pioneer investigation for comprehension of the full plasticity is due to Mesarovic and Fleck [14]. These authors defined two regimes for the full plasticity, finite deformation, and plastic similarity. The transition among them depends on the ratio E/Y, as previously demonstrated in **Figure 4**. A more detailed description can be seen in the work done by Alcalá and Esqué-de los Ojos [15]. For the current purpose, only a general description will be presented (**Figure 5**), for a perfectly plastic material ($n \rightarrow 0$) with specific properties.

In **Figure 5** it is possible to clearly observe the existence of three regions. Firstly, the C factor increases as the contact radius increases. This will happen up to a characteristic value, which depends on the ratio E/Y. The second region is one in which there is a drop in the C values, typical to simulate perfectly plastic materials, in which one would expect in fact a constant value. In [15] one can see that the plasticity theory applied to the simulation (deformation theory vs. flow plasticity theory) affects the description of this region (topic beyond the scope of this chapter). Finally, there is a third regime, in which the constraint factor backs to increase with increasing loading. This regime will be explained in detail further.

An effect that helps explain the fall in C factor with the a/D was demonstrated by Mesarovic and Fleck [14], verifying that there is lack of uniformity of the vertical speed at which the material experiences as the contact radius increases. In other words, this means that the friction between the sphere and the plane should be considered to provide a more realistic simulation.

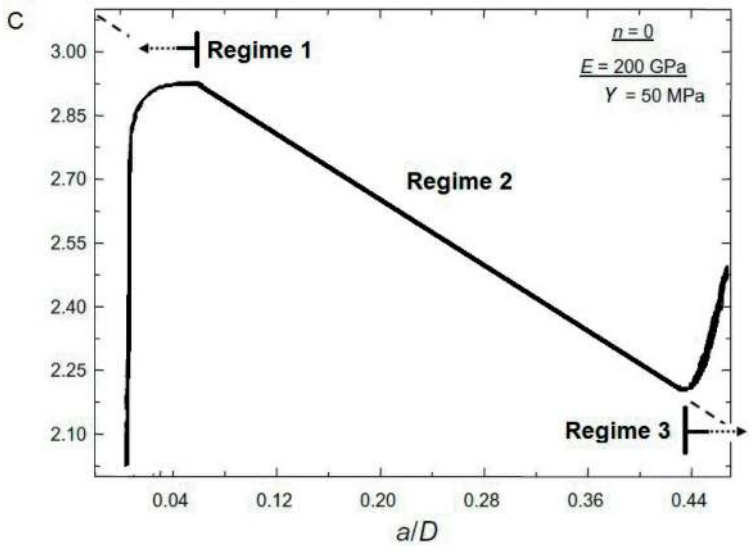

Figure 5. Variation of constraint factor with ratio a/D (Adapted from [15]).

Alcalá and Esqué-de los Ojos [15] consider a friction coefficient value of 0.07 as ideal for property extraction from a spherical indentation test. The effect of friction described in [14] can be seen in **Figure 6**.

Moreover, Alcalá and Esqué-de los Ojos [15] commented on the difficulty of any experimental support existence to prove the decay in C. According to these authors, the reasons for this are related to the strain hardening, being:

i. Metals with low work-hardening exponent generally have sufficiently high yield stress, such that the increase occurring in C takes place within a broad range, which limits the occurrence of hardness drop with high values of a/R

ii. The frictional effects are significant enough to lower work-hardening exponent values, such that an increase in hardness occurs, while the decay is not observed.

While this experimental evidence is not presented, the simulation results generated a series of equations for region 2 of **Figure 5** (the decay). **Figure 7** shows a comparison among some of these equations, for the variation of C with a/R.

The last regime inserted into the full plasticity of a perfectly plastic material can be defined as a physical limit for the mechanical contact existence. This phenomenon can be treated as a "decoupling" of the contact. **Figure 8** helps to explain better the phenomenon.

Figure 8A shows the geometry of the sphere-plane contact, indicating a depth δ that varies in conjunction with the contact radius for a same radius R or diameter D. It is possible to relate the variation of the a/D ratio with δ/A by means of simple geometry, and this variation is shown in **Figure 8B** for a ball diameter with D = 3 mm. One can see that δ/a ≈ a/D for a certain

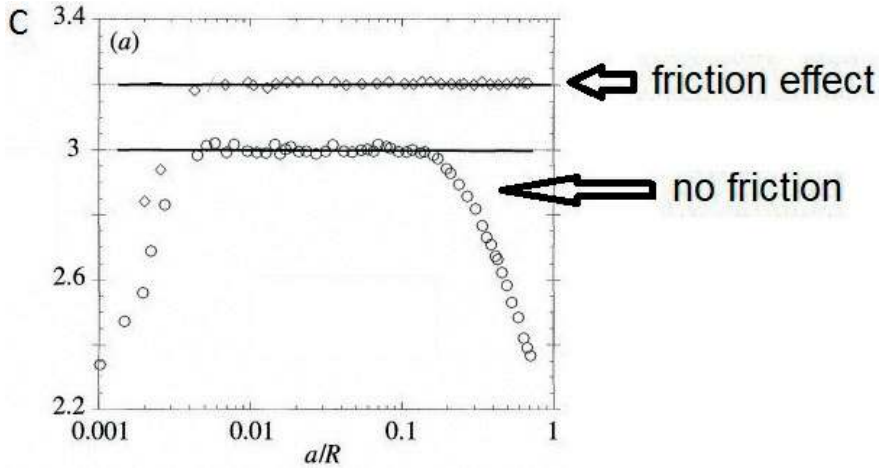

Figure 6. Variation of constraint factor with ratio a/R for a material with E/Y = 10,000 and Poisson's ratio of 0.3, with and without friction (Adapted from [14]).

value, there is a small deviation thereafter. Thus, increments above a certain value mean a geometric inconsistency, in which the ball cannot make a suitable contact with the plane in the axial direction of loading, representing a "decoupling" of the contact, which would entail artificially greater contact pressures (proportionally smaller radius values) as shown in **Figure 5**.

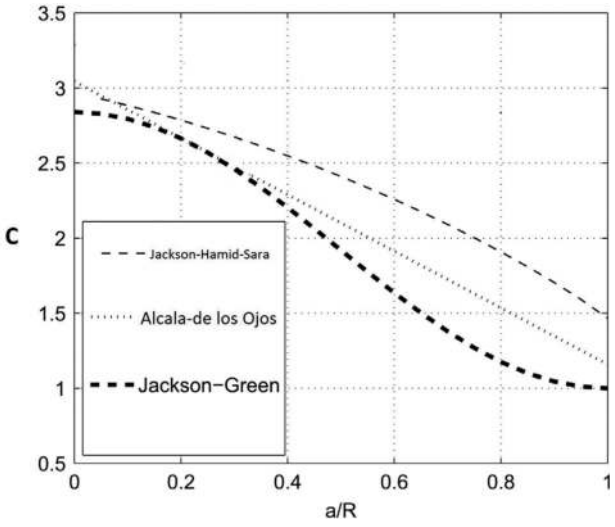

Figure 7. Equations to describe the finite deformation regime for a perfectly plastic material: Jackson-Green [16], Alcalá et al. [17], and Jackson et al. [18] (Adapted from [19]).

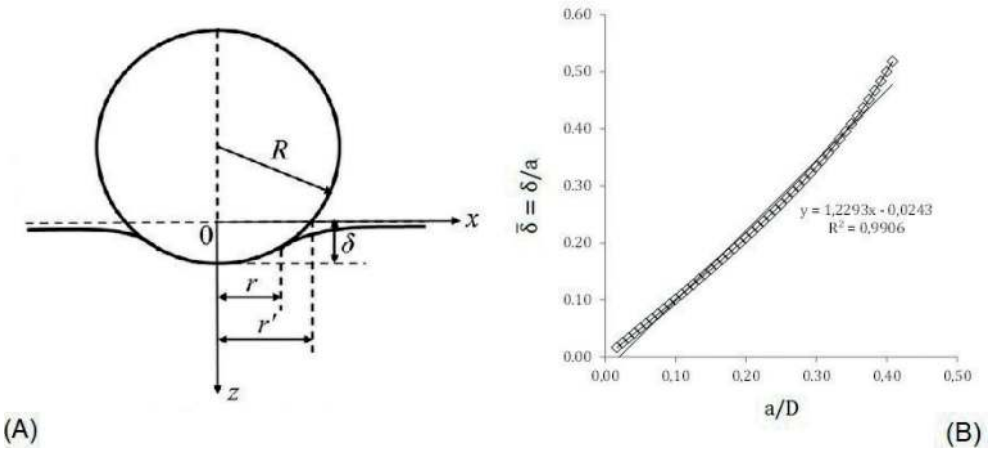

Figure 8. (A) Detailed geometry of sphere-plane contact and (B) variation of normalized depth with the normalized contact radius (Adapted from [12]).

5. Hardening effects

The hardening of metals was incorporated into Tabor's concept, through work-hardening exponent (n). To the full plasticity regime, empirical equations can be derived to compute the effect of this property in the constraint factor. This type of relationship was shown, for example, by Matthews [20] and subsequently reviewed by Sundararajan and Tirupataiah [21], who demonstrated it for a wider range of experimental points.

Although these formulations may be useful from a practical point of view, here it is relevant to present in what deformation regime during the mechanical contact the work-hardening can alter the behavior. The example presented by Komvopoulos and Song [12] for a material with E/Y = 11 (**Figure 9**) makes it interesting for that.

It is noticed that the work-hardening exponent changes with great intensity of the C values in the full plasticity regime. Thus, the differential hardness value will be affected by the work hardening, as will be discussed in the next section.

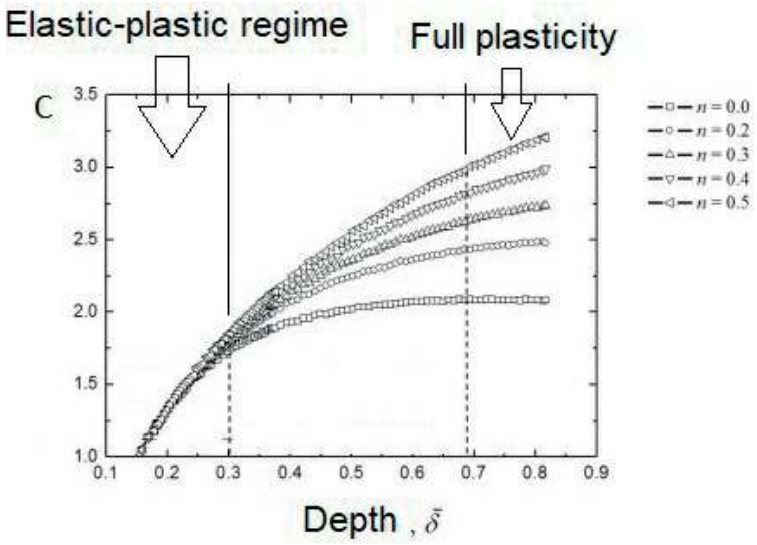

Figure 9. Variation of constraint factor with normalized depth for a material with E/Y = 11, for different work-hardening exponents (Adapted from [12]).

6. Experimental evaluation of differential hardness and trends in numerical simulation

An experiment to certify the existence of the differential hardness as predicted by Tabor is not a simple task. Jamari and Schipper [22] made an important attempt for that. These researchers used SiC as rigid plane, in which copper or aluminum balls were pressed against it.

Whereas deformation profiles plotted after the test, it was shown that the hardness difference for the case of Cu would be 1.33 and 1.39 for the case of Al, much lower than that established by Tabor (2.5).

Perhaps, for this reason, the results were the scenes of further discussion. Jackson and Green [23] criticized especially the method of measuring the deformation by profilometry after removal of the load and the effect of hardening. Jamari and Schipper [24] argued explaining the measuring method for the profile of spheres before the test and the approximation of the profile thereof after deformation. About hardening, they provided values showing the increasing of sphere hardness, which was relatively insignificant.

The experimental demonstrations for differential hardness remain scarce, especially for the boundary conditions given by Alcalá and Esqué-de los Ojos [15] in the abovementioned. These can be considered as inherent challenges to the contact mechanics in its present state of the art.

In this line, the work presented by Ghaednia et al. [19] sheds light to the theories discussed here, with a new numerical limit for the occurrence of differential hardness in the sphere-plane contact.

The first important question raised by these authors, also discussed by Jamari and Schipper [22], is the effect to consider if the load is being applied either on the plan or on the sphere. For that, Ghaednia et al. [19] make it clear what equation to adopt for each case, being adopted the Jackson-Green expression [16] for plane hardness and the Jackson et al. one [18] for the ball hardness.

From this, each equation is then used to calculate a stress ratio (Y*), equivalent to the differential hardness:

$$Y^* = {}^{Y_B}/_{Y_M} \tag{3}$$

By selecting different combinations of properties for sphere and plane, these authors got simulated for what value the constraint factor presents with no further changes, within the full plasticity regime for the plane. The found value for the differential hardness is equivalent to 1.7, 32% lower than that predicted by Tabor.

7. Conclusions and final remarks

The main contributions in the field of contact mechanics were demonstrated along this chapter applied for an important specific system, sphere-plane contact, in which several hardness tests are performed.

Clearly, there is a lack in the experimental demonstration of theories presented. This is an interesting challenge, as the numerical simulation increases at much higher speed than the experimental results.

An updated value obtained through numerical simulation for the differential hardness is 1.7, different from that predicted by Tabor (2.5). Certainly, an experimental demonstration could be elucidating this difference.

In addition, the hardening and friction effects on the sphere-plane system can be more explored through both numerical simulations and experimental arrangements.

Acknowledgements

The author thanks CNPq, through Project 312385/2014-5.

Nomenclature

a	Contact radius
c	Radius of plastically affected zone
C	Constraint factor
D	Sphere diameter
E	Elastic modulus
H	Hardness
n	Work-hardening exponent
p_M	Mean contact pressure
R	Sphere radius
Y	Yield stress
Y*	Ratio between yield stress of sphere and plane
Y_B	Yield stress of sphere
Y_M	Yield stress of metal
z	Depth from the surface
δ	Deflected depth
τ_{max}	Maximum shear stress
ν	Poisson's ratio

Author details

Giuseppe Pintaude

Address all correspondence to: giuseppepintaude@gmail.com

UTFPR – Federal University of Technology, Paraná, Brazil

References

[1] Hertz H. On the contact of elastic solids. Journal für die reine und angewandte Mathematik. 1881;**92**(156-171):110

[2] Mackerle J. Finite element and boundary element simulations of indentation problems: A bibliography (1997-2000). Finite Elements in Analysis and Design. 2001;**37**(10):811-819

[3] ASTM E10-15. Standard Test Method for Brinell Hardness of Metallic Materials. In: ASTM International. editor. West Conshohocken, PA: ASTM; 2015

[4] Song J, Ma L, Low SR. Finite-element modeling and experimental comparisons of the effects of deformable ball indenters on Rockwell B hardness tests. Journal of Testing and Evaluation. 2003;**31**(6):1-10

[5] Tabor D. The hardness of solids. Review of Physics in Technology. 1970;**1**(3):145-179

[6] Johnson KL, editor. Contact Mechanics. Cambridge: Cambridge University; 1985

[7] Shaw MC, de Salvo GJ. On the plastic flow beneath a blunt axisymmetric indenter. Journal of Manufacturing Science and Engineering. 1970;**92**(2):480-492

[8] Green I. Poisson ratio effects and critical values in spherical and cylindrical Hertzian contacts. International Journal of Applied Mechanics and Engineering. 2005;**10**(3):451-462

[9] Pintaude G. Analysis of spherical contact models for differential hardness as a function of Poisson's ratio. Journal of Tribology. 2015;**137**(4):044502

[10] Giannakopoulos AE, Suresh S. Determination of elastoplasctic properties by instrumented sharp indentation. Scripta Materialia. 1999;**40**(10):1191-1198

[11] Bishop RF, Hill R, Mott NF. The theory of indentation and hardness tests. The Proceedings of the Physical Society. 1945;**57**(3):147-159

[12] Song Z, Komvopoulos K. Elastic–plastic spherical indentation: Deformation regimes, evolution of plasticity, and hardening effect. Mechanics of Materials. 2013;**61**:91-100

[13] Megalingam A, Mayuram MM. A comprehensive elastic-plastic single-asperity contact model. Tribology Transactions. 2014;**57**(2):324-335

[14] Mesarovic SD, Fleck NA. Spherical indentation of elastic–plastic solids. Proceedings of the Royal Society of London. Series A. 1999;**455**:2707-2728

[15] Alcalá J, Esqué-de Los Ojos D. Reassessing spherical indentation: Contact regimes and mechanical property extractions. International Journal of Solids and Structures. 2010; **47**(20):2714-2732

[16] Jackson RL, Green I. A finite element study of elasto-plastic hemispherical contact against a rigid flat. Journal of Tribology. 2005;**127**(2):343-354

[17] Alcalá J, Barone AC, Anglada M. The influence of plastic hardening on surface deformation modes around Vickers and spherical indents. Acta Materialia. 2000;**48**(13):3451-3464

[18] Jackson RL, Ghaednia H, Pope S. A solution of rigid–perfectly plastic deep spherical indentation based on slip-line theory. Tribology Letters. 2015;**58**(3):1-7

[19] Ghaednia H, Pope S, Jackson RL. A comprehensive study of the elasto-plastic contact of a sphere and a flat. Tribology International. 2016;**93**:78-90

[20] Matthews JR. Indentation hardness and hot pressing. Acta Metallurgica. 1980;**28**(3):311-318

[21] Sundararajan G, Tirupataiah Y. The hardness-flow stress correlation in metallic materials. Bulletin of Materials Science. 1994;**17**(6):747-770

[22] Jamari J, Schipper DJ. Experimental investigation of fully plastic contact of a sphere against a hard flat. Journal of Tribology. 2006;**128**(2):230-235

[23] Jackson RL, Green I. Discussion: Experimental Investigation of Fully Plastic Contact of a Sphere Against a Hard Flat (Jamari J, Schipper DJ, 2006, ASME J Tribol, 128, pp. 230–235). Journal of Tribology. 2007;**129**(3):700

[24] Jamari J, Schipper DJ. Closure to Discussion of Experimental Investigation of Fully Plastic Contact of a Sphere Against a Hard Flat (2007, ASME J Tribol, 129, p. 700). Journal of Tribology. 2007;**129**(3):701